Received: 14 September 2021 | Revised: 4 October 2021 | Accepted: 4 October 2021

DOI: 10.1111/gtc.12899

Genes to Cells WILEY

ORIGINAL ARTICLE

Planar cell polarity protein Vangl2 and its interacting protein Ap2m1 regulate dendritic branching in cortical neurons

Misato Yasumura[1,2] | **Akari Hagiwara**[1] | **Yamato Hida**[1] | **Toshihisa Ohtsuka**[1]

[1]Department of Biochemistry, Faculty of Medicine, University of Yamanashi, Chuo, Japan

[2]Department of Anatomy and Neuroscience, Graduate School of Medicine, Osaka University, Suita, Japan

Correspondence
Toshihisa Ohtsuka, Department of Biochemistry, Graduate School of Medicine/Faculty of Medicine, University of Yamanashi, 1110 Shimokato, Chuo, Yamanashi 409-3898, Japan.
Email: tohtsuka@yamanashi.ac.jp

Present address
Akari Hagiwara, Department of Applied Biological Science, Faculty of Science and Technology, Tokyo University of Science, Noda, Japan

Funding information
Japan Society for the Promotion of Science, Grant/Award Number: KAKENHI/17K14949 and KAKENHI/19H03324

Communicated by: Tadashi Uemura

Abstract

Van Gogh-like 2 (Vangl2) is a mammalian homolog of *Drosophila* core planar cell polarity (PCP) protein Vang/Strabismus, which organizes asymmetric cell axes for developmental proliferation, fate determination, and polarized movements in multiple tissues, including neurons. Although the PCP pathway has an essential role for dendrite and dendritic spine formation, the molecular mechanism remains to be clarified. To investigate the mechanism of Vangl2-related neuronal development, we screened for proteins that interact with the Vangl2 cytosolic N-terminus from postnatal day 9 mouse brains using a yeast two-hybrid system. From 61 genes, we identified adaptor-related protein complex 2, mu 1 subunit (Ap2m1) as the Vangl2 N-terminal binding protein. Intriguingly, however, the pull-down assay demonstrated that Vangl2 interacted with Ap2m1 not only at its N-terminus but also at the C-terminal Prickle binding domain. Furthermore, we verified that the downregulation of Ap2m1 in the developing cortical neurons reduced the dendritic branching similar to what occurs in a knockdown of Vangl2. From these results, we suggest that the membrane internalization regulated by the PCP pathway is required for the developmental morphological change in neurons.

KEYWORDS

adaptor-related protein complex, PCP, Van Gogh-like proteins, yeast two-hybrid

1 | INTRODUCTION

Van Gogh (Vang), also known as Strabismus (Stbm), was originally identified in *Drosophila* as a core planar cell polarity (PCP) protein, which when mutated causes considerable misorientation of organized epithelial structures (Tissir & Goffinet, 2013; Torban et al., 2004). Vang/Stbm is evolutionarily conserved and can be seen in several species including insects, fish, and mammals. Mice have two Vang/Stbm family members: Van Gogh-like protein (Vangl) 1 and Vangl2, whose mRNAs are expressed in the developing and adult nervous system (Tissir & Goffinet, 2006). Mutations in *VANGL* genes have been identified in sporadic and familial cases of neural tube defects in humans, and similar defects have been found in the *looptail* (*Lp*) mouse mutant that has mutations in Vangl2.

Vangl2 is a membrane protein comprising four transmembrane domains and two intracellular domains, one each at the amino (N)- and carboxyl (C)-terminals. The C-terminus has multiple domains including the PDZ-binding

motif, the Prickle binding domain (PkBD), and some missense mutations that cause the *Lp* mutant (Torban et al., 2004). Indeed, two independent *Lp* mutations in Vangl2 have been shown to impair interactions with Dvl proteins, which suggests that Vangl2-Dvl-mediated signaling underlies the neural tube defect (Torban et al., 2004). In the nervous system, Vangl2 regulates commissural axon growth-cone guidance by antagonizing Dvl-mediated signaling (Shafer et al., 2011). Additionally, the Vangl2 PDZ-binding motif is tightly associated with postsynaptic density (PSD)-95 protein. They form a protein complex with NMDA receptors, Prickle2, and N-cadherin, which regulate the clustering of postsynaptic molecules and dendritic spine formation (Nagaoka & Kishi, 2016; Nagaoka, Ohashi, et al., 2014; Nagaoka et al., 2015; Yoshioka et al., 2013). Intriguingly, the Vangl2 C-terminal deletion mutant was shown to enhance dendritic branching, whereas the N-terminus deletion mutant reduced both spine density and dendritic branching (Hagiwara et al., 2014), which indicates that Vangl2 has an essential role in modulating the constitution of neuronal morphology.

Vangl2 plays critical roles in early neural development and axon/dendritic branching. However, despite these broad-ranging functions, the functional domains and proteins that it interacts with (other than PCP proteins) have not been well studied. Unlike the well-characterized domains of the C-terminal region, which include a region that interacts with PCP partner proteins (Bailly et al., 2018), the roles of the N-terminal region remain poorly characterized. Here, we identified proteins that interact with the N-terminus of Vangl2 (Vangl2N) using yeast two-hybrid screening. Following the pull-down assay, we found proteins that interact with Vangl2: adaptor-related protein complex 2, mu1 subunit (Ap2m1), eukaryotic translation elongation factor 1 α1 (Eef1a1), and Ras/Rap GTPase-activating protein SynGAP (SynGAP1). Ap2m1 was found to be the most likely one to interact with Vangl2N, binding to both the N-terminus and the C-terminal PkBD. Remarkably, knockdown (KD) of Ap2m1 results in less branching of cortical neurons, similar to what happens in the KD of Vangl2. Because the AP2 protein regulates membrane internalization via clathrin-mediated endocytosis (CME), the Vangl2-involved PCP signal coordinates the temporal and spatial regulation of neuronal morphology.

2 | RESULTS

2.1 | Screening of novel proteins that interact with Vangl2

To search for novel Vangl2-binding proteins, we conducted yeast two-hybrid screening with the N-terminal region (amino acid 1–114, Vangl2N) as bait and mated it with a postnatal day 9 (P9) mouse brain cDNA library containing the Y187 yeast strain (Figure 1a,b). The resulting diploid cells were screened on different stringency plates, and approximately 4.5×10^7 diploid cells were cultured. Among 213 positively identified clones, we identified 61 genes by sequencing and BLAST searches (Figure 1b, Table 1). To investigate how the N-terminal region of Vangl2 regulates dendrites and/or dendritic spine formation, we selected 10 proteins from those that were identified, choosing them based on proteomic data from PSD proteins in the P9 mouse cortex (Shao et al., 2017) (Table 1 indicated by *). Among them, two housekeeping proteins, one nuclear protein, and two presynaptic proteins were excluded from further analysis. As for the remaining five proteins, Ap2m1, ATPase Na^+/K^+ transporting subunit β1 (Atp1b1), Eef1a1, kinesin family member 1A (Kif1a), and SynGAP1, we examined how they interacted with the N-terminal region of Vangl2. We performed pull-down assays using purified GST-Vangl2N and GST-Vangl2C (amino acid 242–521) with cell lysates from HEK293T cells that expressed amino-terminally FLAG-tagged protein. Cell lysates expressing FLAG-Ap2m1 or FLAG-SynGAP1 were mostly retained on GST-Vangl2N, with fewer retained on GST-Valng2C. Conversely, cell lysates expressing Eef1a1 interacted with both GST-Vangl2N and GST-Vangl2C, whereas those expressing Atp1b1 and Kif1a were retained the least (Figure 1c, Table 2). As neurons develop, precise sorting and/or intake of cargoes should be essential for neural branching regulated by the PCP pathway. The AP-2 complex is known to be involved in the intake of cargoes—clearing AMPA and Eph receptors from the cell surface—and the control of the synaptic transmission. Among the proteins we identified, Ap2m1 is a medium heterotetramer subunit of the AP-2 complex, comprising two large α and β subunits (Ap2a1/Ap2a2, Ap2b1) and a small subunit (Ap2s1) (Koscielny et al., 2018). Considering the amount of pulled down FLAG-tagged protein, and previous findings that depletion of Ap2m1 and Ap2b1 impairs axonal and dendritic development, respectively (Koscielny et al., 2018; Kyung et al., 2017), we focused on Ap2m1 for further analysis.

2.2 | The region of Vangl2 that interacted with Ap2m1

Yeast two-hybrid screening allowed us to isolate four independent cDNA clones encoding Ap2m1. These clones contained fragments of Ap2m1 that encoded the amino acids 232–367, 198–324, 224–363, and 195–367. To examine whether the fragment of Ap2m1 that encoded the amino acids from 195 to 367 was sufficient for binding to

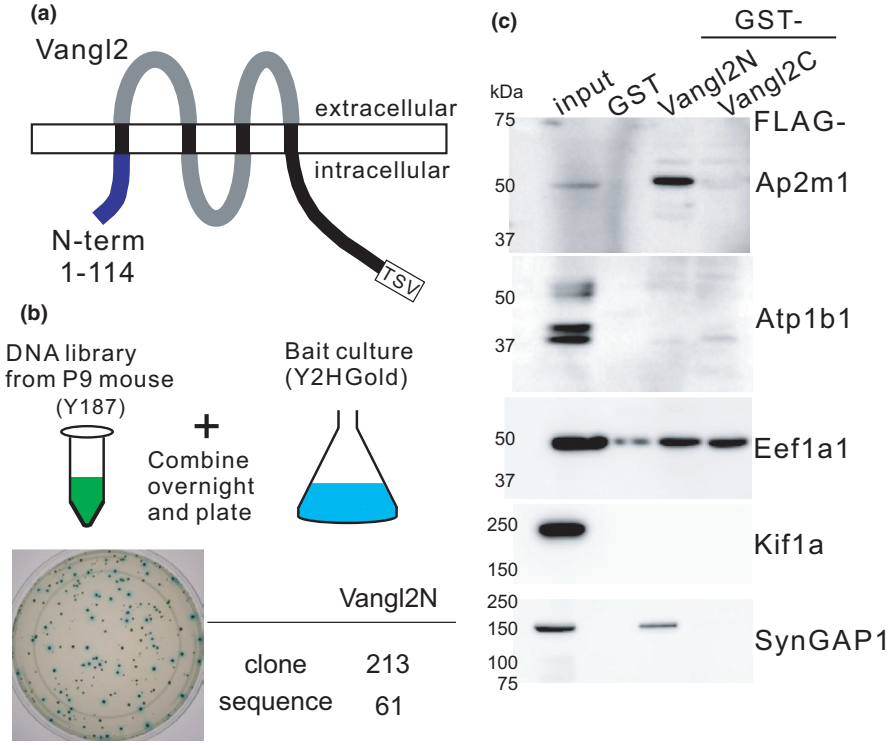

FIGURE 1 Screening of Vangl2 interacting partners using yeast two-hybrid. (a) Structure of the Vangl2 protein includes four transmembrane regions (black boxes, 111–126, 148–166, 183–202, and 218–237), and a PDZ binding motif (TSV, 519–521). To detect novel Vangl2 interacting partners, the N-terminal (1–114) region of Vangl2 was incorporated as the bait plasmid. (b) The bait culture of Vangl2N was combined with prey plasmids of the P9 mouse DNA library and then plated. The positive clones were identified via blue color staining. (c) Pull-down assays using purified GST-Vangl2N and GST-Vangl2C (amino acid 242–521) and cell lysates from HEK293T cells that expressed FLAG-tagged proteins. From the five postsynaptically localized proteins, Ap2m1 and synGAP1 are bound strongly to the N-terminal region rather than the C-terminal region of Vangl2. The full-length western blots are presented in Figure S2

the N-terminal region of Vangl2, we performed pull-down assays using purified GST-Ap2m1 (195-367aa) with cell lysates from HEK293T cells that expressed the amino-terminally HA-tagged Vangl2 deletion mutant. Cell lysates from HEK293T cells that expressed HA-Vangl2 or Vangl2 lacking the C-terminal region (Vangl2ΔC) were retained on GST-Ap2m1 (195–367aa) (Figure 2a,b). The interaction of the Ap2m1 fragment with Vangl2 was also observed in HEK293T cells co-transfected with EGFP-tagged Ap2m1 fragments and HA-tagged Vangl2 (Figure 2c). These results indicated that the region of Ap2m1 that encodes the amino acids from 195 to 367 was sufficient for the interaction with Vangl2. Unlike the results in Figure 1c, Vangl2ΔN was retained on GST-Ap2m1 (195-367aa) from cell lysates expressing HA-Vangl2ΔN (Figure 2a,b). To identify the region of Vangl2 responsible for the interaction with Ap2m1, we performed pull-down assays with multiple regions using purified GST-Vangl2 fragments and cell lysates from HEK293T cells that expressed FLAG-Ap2m1 (Figure 3a). GST-Vangl2-1 and GST-Vangl2N retained FLAG-Ap2m1 from the cell lysates, but GST-Vangl2-2 did not (Figure 3b). Similarly, GST-Vangl2C and GST-Vangl2-4, but not GST-Vangl2-, 3, −4, −5, or −6 retained FLAG-Ap2m1 from the cell lysates (Figure 3b). The amount of pulled down FLAG-Ap2m1 via GST-Vangl2-1 was more than that via GST-Vangl2-4. These results suggested that Ap2m1 binds strongly to Vangl2 through the N-terminal 1-65aa region and binds weakly through the C-terminal 298-382aa region, which corresponds to the PkBD.

2.3 | The functional role of Ap2m1 in neuronal dendritic branching

From the yeast two-hybrid screening, we found an association between Vangl2 and the adaptor-related protein complex, AP2. To evaluate the role of AP2 on the morphology of neurons, an shRNA construct was designed to downregulate endogenous Ap2m1. The efficiency of Ap2m1 shRNA was first confirmed by transfection in HEK293T cells (Figure 4a,b). Next, we electroporated the Ap2m1 shRNA construct with EGFP into embryonic cortical neurons (E14.5–15.5). At P21, we characterized the

TABLE 1 Genes identified from Y2H using Vangl2N

	Gene symbol	Name	Synaptic localization (pre/post-synaptic)
(1) Receptors, channels, and transporters			
1	Astn1	astritactin 1	
2	Atp1b1*	ATPase, Na/K transporting, beta 1 polypeptide	post
3	Atp1b2	ATPase, Na/K transporting, beta 2 polypeptide	
4	Gria1	Glutamate receptor 1	
5	Grip2	glutamate receptor interacting protein 2	
(2) Scaffold, adaptor, and membrane-trafficking proteins			
6	Ap2m1*	adaptor-related protein complex 2, mu 1 subunit	pre/post
7	Pclo*	protein piccolo	pre
8	Syt2	synaptotagmin−2	pre
9	Syt4	synaptotagmin−4	pre/post
10	Syt7*	synaptotagmin−7	pre
11	Syt11	synaptotagmin−11	post
(3) Kinases/phosphatases and regulators			
12	Ctdnep1	CTD nuclear envelope phosphatase 1	
13	Ptprm	receptor-type tyrosine-protein phosphatase mu	
(4) Small G-proteins, GTPase, ATPase, and regulators			
14	Syngap1*	Ras/Rap GTPase-activating protein SynGAP	post
(5) Motor proteins			
15	Clstn1	calsyntenin1	pre/post
16	Kif1a*	kinesin family member 1A	pre/post
(6) Cell adhesion proteins			
17	Cadm3	cell adhesion molecule 3, syncam 3	pre
18	Ctnnd1	catenin, delta 1	pre/post
19	Itga6	integrin alpha 6	
20	Ncam2	neural cell adhesion molecule 2	
21	Pcdh1	protocadherin 1	
22	Pcdha2	protocadherin alpha 2	
23	Pcdhgc3	protocadherin gamma subfamily C, 3	
24	Pecam1	platelet endothelial cell adhesion molecule	
25	Pvrl2	nectin cell adhesion molecule 2	
26	Pvrl3	nectin cell adhesion molecule 3	
(7) Chaperone/folding proteins			
27	Dnaja1	DnaJ Hsp40 member A1	
28	Fkbp1b	FK506 binding protein 1b	
(8) Metabolism-related proteins			
29	B4galnt1	beta−1,4-N-acetyl-galactosaminyl transferase 1	
30	Cds1	CDP-diacylglycerol synthase 1	
31	Gapdh*	Glyceraldehyde−3-phosphatase dehydrogenase	
32	Masp1	mannan-binding lectin serine peptidase 1	
33	Pomgnt1	protein O-linked mannose beta−1,2-N-acetylglucosaminyltransferase 1	
34	Ube2m	NEDD8-conjugating enzyme Ubc 12	

(Continues)

TABLE 1 (Continued)

	Gene symbol	Name	Synaptic localization (pre/post-synaptic)
(9) Mitochondrial proteins			
35	Timm23	mitochondrial import inner membrane translocase subunit Tim23	
(10) Transcription/translation/ribosomal proteins			
36	Eef1a1*	eukaryotic translation elongation factor alpha 1	post
37	Gltf3c5	general transcription factor IIIC, polypeptide 5	
38	Klf13	kruppel-like factor 13	
39	Mkl2	myocardin related transcription factor B	
40	Pcbp2*	poly(rC) binding protein 2	
41	Scaf8	SR-related and CTD-associated factor 8	
42	Zmiz1	zinc finger MIZ domain-containing protein 1	
43	Zmiz2	zinc finger MIZ domain-containing protein 2	
44	2700060E02Rik(Rtraf)	RNA transcription, translation and transport factor	
(11) DNA/nucleus/histone proteins			
45	Hnmph3	heterogeneous nuclear ribonucleoprotein H3	
46	Hnmpul1	heterogeneous nuclear ribonucleoprotein U-like 1	
47	H1fx	H1.10 linker histone	
48	Nrbp1	nuclear receptor binding protein 1	
49	Papola	poly A polymerase alpha	
50	Papolb	poly A polymerase beta	
(12) Others			
51	Anapc10	anaphase promoting complex subunit 10	
52	Atg2b	autophagy related 2b	
53	Efr3b	EFR homolog B	post
54	Hdlbp	high density lipoprotein binding protein	
55	Kpna6	karyopherin alpha 6	
56	Nrep	neuronal regeneration related protein	
57	Tmem98	transmembrane protein 98	
58	Tmem132a	transmembrane protein 132a	
59	Ywhaz*	14–3–3 protein zeta/delta	
60	Zfyve9	zinc finger FYVE domain-containing protein	
61	2510009E07Rik		

*Proteins identified from the postsynaptic density of the P9 mouse cortex.

TABLE 2 Pulldown assay for the Vangl2 N- and C-terminal

	Gene symbol	Name	MW (kDa)	Vangl2N	Vangl2C
1	Atp1b1	ATPase Na/K transporting 1 polypeptide	35	+	+
2	Ap2m1	adaptor-related protein complex 2, mu1 subunit	50	+++	+
3	Eef1a1	eukaryotic translation elongation factor alpha1	50	++	++
4	Syngap1	Ras/Rap GTPase-activating protein synGAP	148	++	-
5	Kif1a	Kinesin family member 1A	202	-	-

Note: -; less interaction, +; less than input, ++; equal to input, +++; more than input

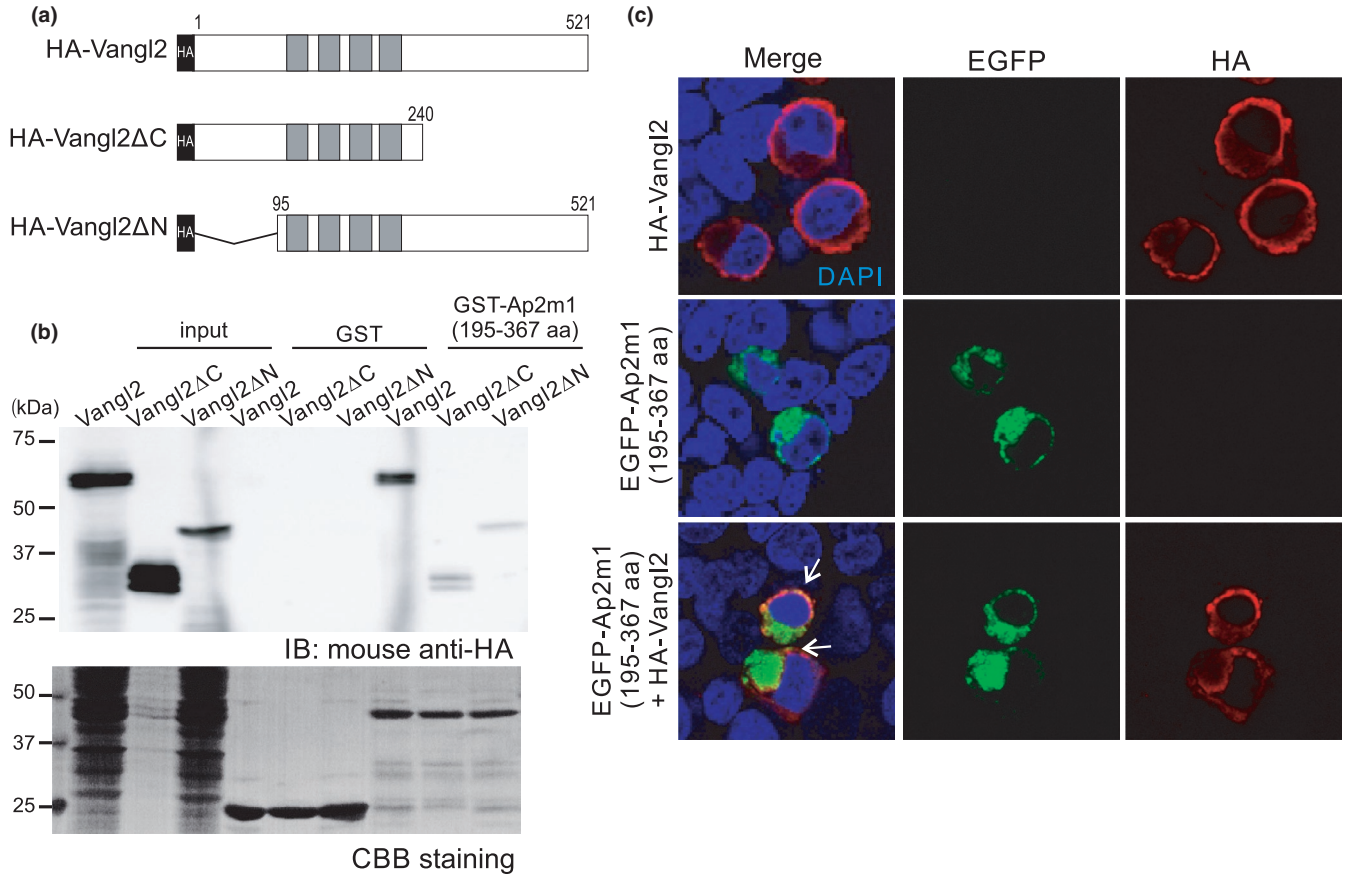

FIGURE 2 Binding of Vangl2 with Ap2m1. (a) Constructs of HA-tagged Vangl2. (b) Pull-down assays using purified GST-Ap2m1(aa 195–367) and cell lysates from HEK293T cells that expressed HA-tagged proteins. Ap2m1 robustly interacted with the full length of Vangl2. However, binding of Ap2m1 was reduced by the deletion of the N-terminal and the C-terminal deletion. (c) Colocalization of Vangl2 and Ap2m1 by confocal microscopy. HA- and EGFP-labeled Vangl2 and Ap2m1 were transfected in HEK293T cells and the expression was observed via confocal microscopy. Co-expression of HA-Vangl2 and EGFP-Ap2m1 revealed the colocalization of these proteins (arrows)

morphology of cortical pyramidal neurons identified with EGFP. The total length of apical and basal dendrites was significantly lower in Vangl2 and Ap2m1 KD neurons than that in control with scramble shRNA (Figure 4c,d, Table 3). Conversely, spine density was higher in Ap2m1 KD neurons compared to the control and Vanlg2 KD (Figure 4e). The total number of tips was significantly lower in Vangl2 and Ap2m1 KD neurons than control; branches at the secondary dendrite were especially devoid of tips (Figure 4f,g). To study the functional interaction between Vangl2 and Ap2m1, endogenous expression of these proteins was evaluated in primary culture neurons (Figure S1). The shRNA constructs for Vangl2 and Ap2m1 significantly suppressed expression of their respective proteins. However, Ap2m1 expression was not significantly affected by Vangl2 KD, or vice versa (Figure S1c). Specifically, although expression of Ap2m1 was slightly suppressed by Vangl2 KD, that of Vangl2 was enhanced in Ap2m1 KD neurons. These results suggest an association between the Vangl2 portion of PCP proteins and an adaptor protein for membrane internalization that might have a role in the dendritic remodeling in neurons, which can affect neuronal development and plasticity.

3 | DISCUSSION

Vangl2 is a core component of PCP proteins, which are involved in cell-signaling that acts to divide and move cells along the tissue axis. Vangl2 comprises four transmembrane regions with both terminals exposed to the cytosol (Figure 1a) (Tissir & Goffinet, 2013; Yoshioka et al., 2013). In a previous report, we showed that Vangl2 is involved in bidirectional regulation of neuronal dendritic branching; a Vangl2N deletion mutant showed a significant reduction in dendritic branching and spine density (Hagiwara et al., 2014). Therefore, in this report, we searched for molecules that interact with Vangl2N to better understand the molecular mechanism underlying neural dendritic development. From the yeast two hybrid screening,

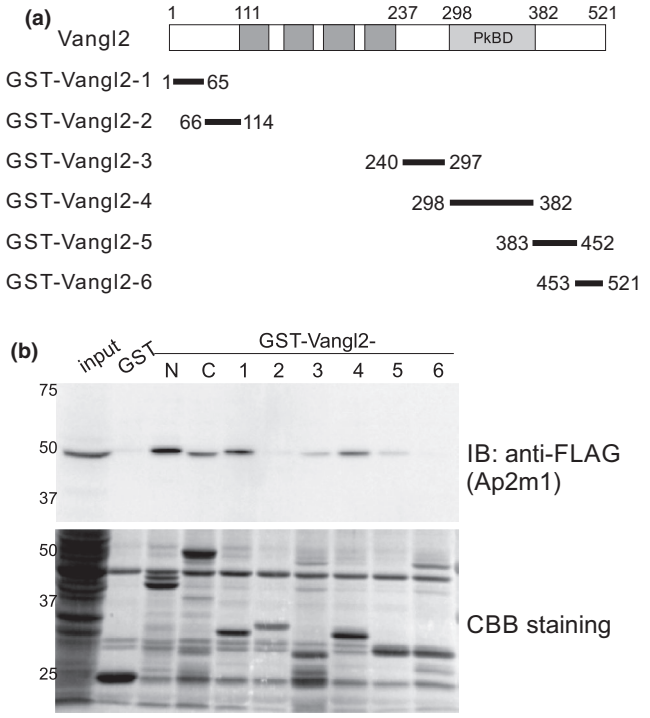

FIGURE 3 Confirmation of the Vangl2-Ap2m1 binding region. (a) Constructs of Vangl2 for GST fusion proteins. The constructs excluded the transmembrane regions (gray boxes from 111 to 237). (b) Pull-down assays using purified GST-tagged each domain of Vangl2 (A) and cell lysate from HEK293T cells that expressed FLAG-Ap2m1. Ap2m1 strongly interacted with the N-terminal (N) and the C-terminal (c). The band could be detected for Vangl2-1 (1–65) and Vangl2, −3, −4, and −5 (240–452), including the Prickle binding domain (PkBD). The PDZ binding motif in Vangl2-6 (453–521) was less essential for the binding of Ap2m1

we obtained 61 candidate genes including pre- and post-synaptic proteins (Table 1) and confirmed the Vangl2N-specific binding to adaptor protein Ap2m1 (Figures 1–3). Furthermore, shRNA KD of Ap2m1 and KD of Vangl2 resulted in less dendritic branching, although spine density increased after Ap2m1 KD (Figure 4). From these results, we suggest that dendritic development associated with the CME could be directed by the PCP pathway.

The C-terminal region of Vangl2 has multiple domains, including the looptail mutations D255E, S464N, and R259L, which cause neural tube defects, as well as interaction sites with numerous proteins, including Prickle (Pk) and PSD-95 (Bailly et al., 2018; Nagaoka et al., 2015; Yoshioka et al., 2013). Binding of Pk2 to the PCP protein binding region (PkBD) of Vangl2 is required for dendritic spine formation (Nagaoka, Ohashi, et al., 2014). Considering synaptic proteins, Vangl2 forms a complex with PSD-95 through a conserved PDZ binding motif, which is required for localization of Vangl2 to the dendritic spines (Yoshioka et al., 2013). Thus, interacting molecules and functional roles of Vangl2 C-terminus have been investigated in terms of neuronal morphology. However, even though the N-terminus has an essential role in neuronal dendritic development, interaction at the N-terminal region has not been well demonstrated (Hagiwara et al., 2014).

In mice, cortical layer 2/3 neurons have immature dendrites at P3, and apical and basal dendrites become longer at P5 and more complex by P15 (Hoshiba et al., 2016). Because Vangl2 expression gradually decreases during this dendritic morphogenesis during the first 1–2 weeks (Yoshioka et al., 2013), we screened molecules interacting with the N-terminal region of Vangl2 using P9 mouse brain cDNA and then identified Ap2m1 as a binding partner. In the pull-down assay using GST-fused Vangl2- and Ap2m1-expressing HEK293T lysates, Ap2m1 is strongly bound to Vangl2N and weakly bound to Vangl2C (Figures 1c and 3b). Consistent with these data, in the pull-down assay using GST-fused Ap2m1- and Vangl2-expressing HEK293T lysates, Ap2m1 is bound to not only Vangl2ΔC but also Vangl2ΔN (Figure 2b). These results suggested that Ap2m1 is preferentially bound to the N-terminus of Vangl2, although it is bound to both the N- and C-terminal regions. A previous study showed that Ap1m1, an AP-1 subunit, binds to the C-terminal YYXXF motif of Vangl2, which is required for Vangl2 transport from the *trans*-Golgi network with the GTP-binding protein, Arfrp1 (Guo et al., 2013). In the present study, we showed that compared with GST-Vangl2-4 (corresponding to PKBD), Ap2m1 preferably interacted with the Vangl2 C-terminal and hardly interacted with GST-Vangl2-3, which contains a YYXXF motif (279-283aa) (Figure 3b). Therefore, the functional role of the interaction between AP-2 and Vangl2C might differ from that between AP-1 and Vangl2C.

Furthermore, in hippocampal neurons, binding of Vangl2 to N-cadherin through PkBD enhances its internalization in a Rab5-dependent manner (Nagaoka, Ohashi, et al., 2014), whereas in epithelial cells, binding to E-cadherin is similar (Nagaoka et al., 2014). Because several endocytic adaptors including AP-2, Dab-2, and Numb associate with E-cadherin for the internalization of CME (Brüser & Bogdan, 2017), AP-2 may play a role in Vangl2-related N-cadherin internalization by binding to Vangl2 and/or N-cadherin.

Because disruption of PCP genes, including Vangl2, Dvl1, and Dapper-antagonist of catenin-1 in mice, causes reduced dendritic arborization in neurons (Hagiwara et al., 2014; Okerlund et al., 2010,2016; Rosso et al., 2005), the Wnt/PCP pathway is essential for the formation of the dendrite, dendritic spine, and excitatory synapse. In this study, we showed that Ap2m1 KD also decreased dendritic length, the total number of tips, and the branch number in cortical neurons and the Vangl2 KD (Figure 4). CME regulated dendritic growth by mediating

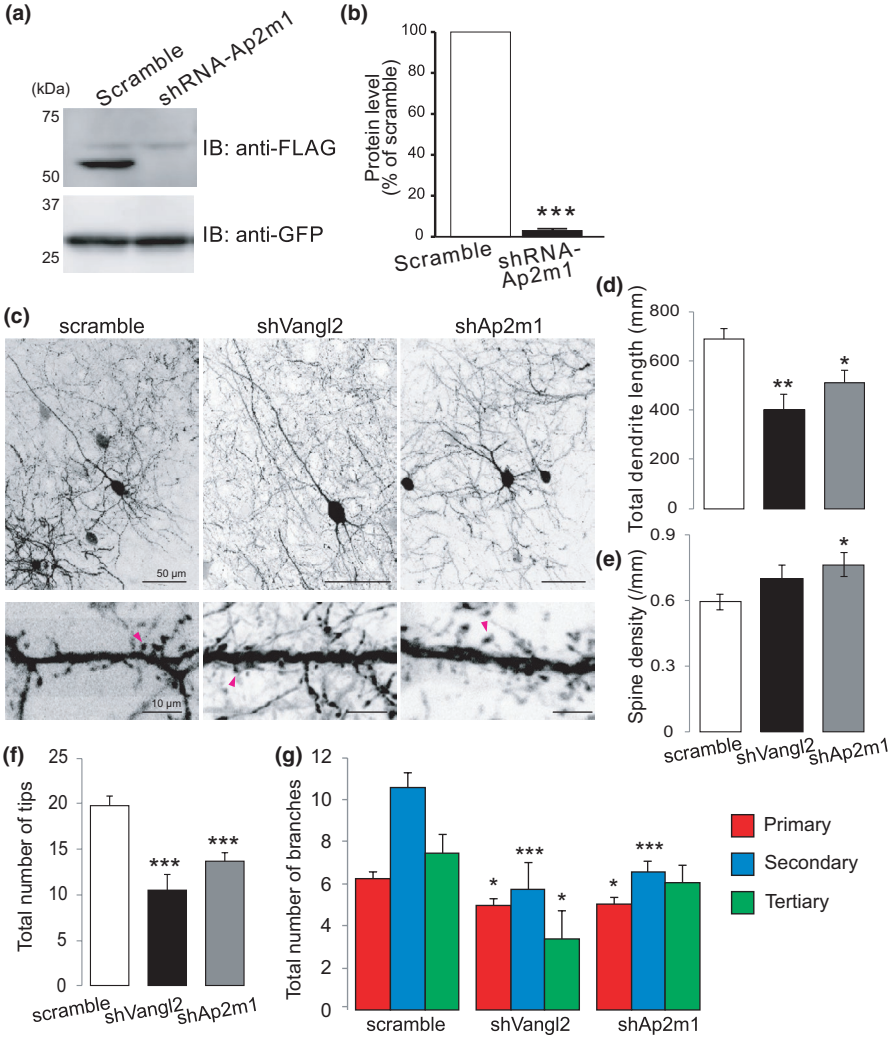

FIGURE 4 Knockdown of Ap2m1 and Vangl2 affects neuronal dendritic branching. (a) Western blot analysis of the KD of shRNA-Ap2m1 on transiently expressed FLAG-Ap2m1 in HEK293T cells. (b) Quantitative data of the Western blot analysis. From three independent tests, the protein level was suppressed about 3.0% ± 0.9%. Data are means ± *SEM*, *** $p < .001$, Student's *t*-test. (c) Morphology of cortical neurons as revealed by co-expressed EGFP with KD vectors. Spine and tip number were measured with high magnification of apical and basal dendrites (bottom, arrowheads). (d–g) The dendritic and spine complexity of neurons expressing the indicated shRNA constructs. Dendritic expansion as measured by total dendrite length was significantly reduced in Vangl2 and Ap2m1 KD neurons, and the spine density was increased in Ap2m1 KD. The number of tips was significantly less in Vangl2 and Ap2m1 KD. Specifically, the numbers of branches on the secondary dendrites were remarkably less in Vangl2 and Ap2m1 KD. Data are means ± *SEM*, *$p < .05$, **$p < .01$ ***$p < .001$, one-way ANOVA post hoc Tukey's test

the internalization of receptors. Indeed, KD of the clathrin assembly protein CALM reduced dendrite length and the overall complexity of the neurites in cultured hippocampal neurons (Bushlin et al., 2008). KD of AP2b1, a subunit of the AP-2 complex, lowered the total number of dendritic tips in rat hippocampal neurons (Koscielny et al., 2018). Here, we further analyzed the functional interaction between Vangl2 and Ap2m1 on neuronal development (Figure S1). Intriguingly, although endogenous Vangl2 KD in the primary culture neuron caused a slight reduction in Ap2m1, Ap2m1 KD increased the expression of Vangl2. From these results, we speculate that Vangl2 partially regulates Ap2m1-related membrane remodeling. The increased Vangl2 expression after Ap2m1 KD also supports the idea that loss of membrane remodeling in Ap2m1 KD neurons facilitates the regulatory PCP pathway. Consistent with these results, the direct interaction between Vangl2 and Ap2m1 suggests that the Wnt/PCP pathway and CME functionally coordinate the development of dendritic morphology.

3.1 | Experimental procedures

The use of animals was approved by the Institutional Committee for the Care and Use of Experimental Animals

TABLE 3 Morphological analysis of the dendritic formation

	Primary	Secondary	Tertiary
Apical dendrite length (μm)			
Scramble	16.5 ± 1.6	57.4 ± 6.6	93.5 ± 19.1
shVangl2	27.3 ± 4.4	45.9 ± 17.4	120.9 ± 26.0
shAp2m1	24.7 ± 3.0	38.0 ± 6.6	58.6 ± 8.5
Basal dendrite length (μm)			
Scramble	21.1 ± 1.5	52.3 ± 4.1	60.8 ± 5.5
shVangl2	21.9 ± 2.6	41.7 ± 5.4	80.7 ± 16.4
shAp2m1	22.6 ± 1.8	40.7 ± 3.8	77.8 ± 15.6

	Total dendrite length (μm)				
	Apical	Basal	Total	Mouse number	Neuron number
Scramble	262.8 ± 29.7	82.7 ± 5.5	690.7 ± 39.9	4	17
shVangl2	183.8 ± 23.4	54.0 ± 8.9	399.6 ± 64.7	2	8
shAp2m1	186.9 ± 25.1	83.5 ± 10.6	508.8 ± 54.9	3	14

Note: Values are means ± *SEM*.

at the University of Yamanashi (protocol #A25-33, #A30-21). All experiments were conducted according to the recommendations in the *Guidelines for Proper Conduct of Animal Experiments* of the Science Council of Japan (2006). This study was carried out in compliance with the AARIVE (Abunak Research: Reporting of In Vivo experiments) guidelines.

3.2 | Yeast two-hybrid screening

We screened a cDNA library from P9 ICR-mouse forebrain for Vangl2-interacting proteins using the Matchmaker Gold Yeast Two-Hybrid System (Clontech) according to the manufacturer's instructions. Briefly, random-primed cDNA was synthesized using polyA$^+$ RNA taken from the P9 ICR-mouse forebrain using the SMART system (Clontech). The cDNA and pGADT7-Rec vector were co-transformed into the Y187 yeast strain (Clontech), which was plated on SD-lacking leucine (SD/-Leu) plates. Transformants were used for each screening. The Vangl2 amino acid residues 1–114 and 252–521 were subcloned into a pGBKT7 DNA-BD vector to yield pGBKT7-Vangl2 (1–114) and pGBKT7-Vangl2 (252–521), which were transformed into a Y2H Gold yeast strain that was plated on SD/-Typ plates. The positive clone was then used to mate with the Y187 transformants and selected on SD/-Leu/-Trp plates supplemented with X-α-Gal and aureobasidin A (SD/-Leu/-Trp/X/A). The positive clones were subsequently selected on SD/-Leu/-Trp/-Ade/-His/X/A plates. The yeast plasmid was transformed into *E. coli* and isolated DNA was sequenced.

3.3 | Construction of expression vectors

The entire coding sequences of mouse, Ap2m1, Atp1b1, Eef1a1, Kif1a, and SynGAP1, were cloned into a pCAII-FLAG vector. The DNA fragment encoding amino acid residues 195–367 of Ap2m1 was amplified by PCR from the pCAII-FLAG-Ap2m1 vector and cloned into pGEX-4T-1 (GE Healthcare) and pCAII-EGFP vectors. The EcoRI-SalI fragment encoding amino acid residues 1–114 of Vangl2 and PCR amplified DNA fragments encoding residues 1–65, 66–114, 240–297, 298–382, 383–452, and 453–521 from Vangl2 were cloned into a pGEX-4T-1 vector.

3.4 | Pull-down assay

GST, GST-Vangl2N, GST-Vangl2C$^{480–521}$ (Yoshioka et al., 2013), GST-Vangl2-1, −2, −3, −4, −5, −6, and GST-Ap2m1(195–367) were expressed in *E. coli* and lysed by sonication on ice. The bacteria lysate was used as a bait to pull down an interactor from the lysate of HEK293T cells (obtained from the RIKEN BioResource Center) that expressed a protein of interest. The lysates of bacteria and HEK293T cells were mixed and incubated for 2 h at 4°C, followed by incubation with Glutathione Sepharose 4B beads (GE Healthcare) overnight at 4°C. After the beads were extensively washed with lysis buffer (20 mM Tris-Cl, pH 7.5, 150 mM NaCl, 0.5 mM EDTA, 1 mM DTT, 1% [w/v] Triton X-100, protease inhibitors [Complete EDTA-free, Roche]), the bound proteins were eluted from the beads by boiling in SDS sample buffer and analyzed by western blotting.

3.5 | Immunohistochemistry

HEK293T cells (obtained from the RIKEN BioResource Center) were transfected with either or both of HA-Vangl2 and EGFP-Ap2m1 for 48 h. Cells were fixed with 4% paraformaldehyde (PFA) and immunostained with the anti-HA antibody. Fluorescent images were taken with confocal microscopy (FV1200, Olympus).

3.6 | Immunoprecipitation

Expression vectors pCAII-HA-Vangl2 and pCAII-FLAG-Ap2m1 were transfected into HEK293T cells. After 2 days, transfected cells were lysed with radioimmunoprecipitation (RIPA) buffer (50 mM Tris-Cl, pH 8.0, 150 mM NaCl, 0.1% SDS, 0.5% sodium deoxycholate, 1% Nonident P-40, protease inhibitors). Soluble fractions were incubated with anti-FLAG for 2 h at 4°C, followed by incubation with Protein G Sepharose beads (GE Healthcare) overnight at 4°C. After the beads were extensively washed with RIPA buffer, the bound proteins were eluted from the beads by boiling in SDS sample buffer and analyzed by western blotting.

3.7 | shRNA

Oligonucleotides were annealed and ligated into BglII/XhoI site of pSUPER.neo+gfp vector (Oligoengine) to yield pSUPER-Ap2m1 vector according to the manufacturer's instructions. The target sequence of shRNA against Ap2m1 was 5′-CAAAGGCACAGCTGATGAAAC-3′. The knockdown efficiency of shRNA was determined in HEK293T cells by cotransfection with pCAII-FLAG-Ap2m1. Three days after transfection, transfected cells were extracted with SDS sample buffer and analyzed by western blotting. The intensities of bands for Ap2m1 were quantified and normalized with those for GFP. The scrambled noneffective shRNA (5′-GAAACGGAAAGCAGGTACG-3′) (Hagiwara et al., 2014) was used as a control.

3.8 | *In utero* electroporation

All experiments were performed in accordance with relevant guidelines including AARIVE. *In utero* electroporation was performed as described previously (Saito & Nakatsuji, 2001; Tab ata & Nakajima, 2001). Briefly, pregnant ICR mice at embryonic day (E)14.5 or E15.5 were anesthetized with 10% pentobarbital solution (0.1ml/10g body weight), and the uterine horns were exposed. Approximately 1–2 μl of DNA solutions (0.5 μg/μl pCAII-EGFP with 1 μg/μl pSUPER-Scramble, pSUPER-Vangl2 (Hagiwara et al., 2014), or pSUPER-Ap2m1) containing 0.01% fast green was injected into the lateral ventricles of embryos using pulled borosilicate glass capillaries (B120F-4; World Precision Instruments). The head of an embryo in the uterus was pinched with a forceps-type electrode (CUY650P5; NEPA Gene) and five square electric pulses (33 V, 50 ms) at intervals of 950 ms were delivered using an electroporator (CUY21E; NEPA Gene). After electroporation, the embryos were returned to the abdominal cavity to allow continuous development.

3.9 | Evaluation of Vangl2 and Ap2m1 expressions in primary neuronal culture

Preparation of primary cultured neurons has been described previously (Hamada et al., 2021). Briefly, hippocampi were dissected from Wistar rat embryonic-day-18 brains and dissociated by papain at 37°C. The neurons were electroporated with either shRNA-scramble, shRNA-Vangl2, or shRNA-Ap2m1 (CUY21E, NEPA Gene), and then plated on poly-D-lysine (PDL)-coated plates. Cultures were maintained for 14 days in a Neurobasal medium containing B-27 supplement and GlutaMAX (Gibco) and kept in an incubator with 5% CO_2 at 37°C.

For western blotting, the cells were washed with PBS, and the lysates were extracted with lysis buffer (20 mM Tris-HCl, pH 7.5, 150 mM NaCl, 0.5 mM EDTA, 1% Triton X-100, and protease inhibitor cOmplete [Roche Diagnostics]). The samples were applied to SDS-PAGE and detected with anti-Vangl2 antibody (Yoshioka et al., 2013) or anti-Ap2m1 antibody (ab75995, abcam). Band intensity was measured by the expanded ImageJ, version Fiji.

3.10 | Histological analysis

Under deep anesthesia, mice were fixed transcardially with 4% PFA in PBS (pH 7.4) at P21. Coronal sections (50 μm) were embedded and images were acquired with confocal laser microscopy (FV-1200, Olympus). Apical and basal dendrites of the cortical layer 2/3 pyramidal neurons were randomly sampled and analyzed using Amira 5.5 software (FEI).

3.11 | Statistical methods

Statistical significance was evaluated by Student's *t*-test or one-way ANOVA followed by *post hoc* Tukey's test. Statistical significance was assumed when $p < .05$.

ACKNOWLEDGEMENTS

This work was supported by JSPS KAKENHI Grant Numbers 17K14949 (to Y.H.) and 19H03324 (to T.O.) and the University of Yamanashi. We thank T. Okazaki, T. Maeda, and all the members of the Ohtsuka Laboratory for their helpful discussions and technical assistance. For revised experiments, we appreciate the support provided by Dr. S. Hamada at the Ohtsuka Lab and Dr. M. Sato from Osaka University. The experiment of *in utero* electroporation was supported by Dr. T. Mori at Shishu University, and Dr. J. Hatakeyama and Dr. K. Shimamura at the Joint Usage/Research Center for Developmental Medicine, IMEG, Kumamoto University. We also wish to thank Adam Phillips, PhD, from Edanz Group (https://en-author-services.edanz.com/ac) for editing a draft of this manuscript.

CONFLICT OF INTEREST

The authors declare that the research was conducted in the absence of any commercial or financial relationships that could be construed as a potential conflict of interest.

AUTHOR CONTRIBUTIONS

MY designed and performed the biochemical and anatomical analysis with the support of AH and YH, and MY and AH drafted the manuscript. TO directed the study and edited the manuscript.

DATA AVAILABILITY STATEMENT

The datasets used and/or analyzed during the current study are available from the corresponding author on reasonable request.

ORCID

Toshihisa Ohtsuka https://orcid.org/0000-0002-1566-1325

REFERENCES

Bailly, E., Walton, A., & Borg, J. (2018). The planar cell polarity Vangl2 protein: From genetics to cellular and molecular functions. *Seminars in Cell & Developmental Biology*, *81*, 62–70.

Brüser, L., & Bogdan, S. (2017). Adherens junctions on the move—membrane trafficking of E-cadherin. *Cold Spring Harbor Perspectives in Biology*, *9*(3), a029140.

Bushlin, I., Petralia, R. S., Wu, F., Harel, A., Mughal, M. R., Mattson, M. P., & Yao, P. J. (2008). Clathrin assembly protein AP180 and CALM differentially control axogenesis and dendrite outgrowth in embryonic hippocampal neurons. *Journal of Neuroscience*, *28*(41), 10257–10271.

Guo, Y., Zanetti, G., & Schekman, R. (2013). A novel GTP-binding protein-adaptor protein complex responsible for export of Vangl2 from the trans Golgi network, *eLife*, *2*, e00160. https://doi.org/10.7554/eLife.00160.001

Hagiwara, A., Yasumura, M., Hida, Y., Inoue, E., & Ohtsuka, T. (2014). The planar cell polarity protein Vangl2 bidirectionally regulates dendritic branching in cultured hippocampal neurons. *Molecular Brain*, *7*, 79. https://doi.org/10.1186/s13041-014-0079-5

Hamada, S., Nagase, M., Yoshizawa, T., Hagiwara, A., Isomura, Y., Watabe, A. M., & Ohtsuka, T. (2021). An engineered channelrhodopsin optimized for axon terminal activation and circuit mapping. *Communication Biology*, *4*, 461. https://doi.org/10.1038/s42003-021-01977-7

Hoshiba, Y., Toda, T., Ebisu, H., Wakimoto, M., Yanagi, S., & Kawasaki, H. (2016). Sox11 balances dendritic morphogenesis with neuronal migration in the developing cerebral cortex. *Journal of Neuroscience*, *36*(21), 5775–5784.

Koscielny, A., Malik, A. R., Liszewska, E., Zmorzynska, J., Tempes, A., Tarkowski, B., & Jaworski, J. (2018). Adaptor complex 2 controls dendrite morphology via mTOR-dependent expression of GluA2. *Molecular Neurobiology*, *55*, 1590–1606.

Kyung, J. W., Cho, I. H., Lee, S., Song, W. K., Ryan, T. A., Hoppa, M. B., & Kim, S. H. (2017). Adaptor Protein 2 (AP-2) complex is essential for functional axogenesis in hippocampal neurons. *Scientific Reports*, *7*, 41620. https://doi.org/10.1038/srep41620

Nagaoka, T., Inutsuka, A., Begum, K., hafiz, K. M. B., & Kishi, M. (2014). Vangl2 regulates E-cadherin in epithelial cells. *Scientific Reports*, *4*, 6940. https://doi.org/10.1038/srep06940

Nagaoka, T., & Kishi, M. (2016). The planar cell polarity protein Vangl2 is involved in postsynaptic compartmentalization. *Neuroscience Letters*, *612*, 251–255.

Nagaoka, T., Ohashi, R., Inutsuka, A., Sakai, S., Fujisawa, N., Yokoyama, M., Huang, Y. H., Igarashi, M., & Kishi, M. (2014). The Wnt/planar cell polarity pathway component Vangl2 induces synapse formation through direct control of N-cadherin. *Cell Reports*, *6*(5), 916–927.

Nagaoka, T., Tabuchi, K., & Kishi, M. (2015). PDZ interaction of Vangl2 links PSD-95 and Prickle2 but plays only a limited role in the synaptic localisation of Vangl2. *Scientific Reports*, *5*, 12916. https://doi.org/10.1038/srep12916

Okerlund, N. D., Kivimae, S., Tong, C. K., Peng, I.-F., Ullian, E. M., & Cheyette, B. N. R. (2010). Dact1 is a postsynaptic protein required for dendrite, spine, and excitatory synapse development in the mouse forebrain. *Journal of Neuroscience*, *30*(12), 4362–4368.

Okerlund, N. D., Stanley, R. E., & Cheyette, B. N. R. (2016). The planar cell polarity transmembrane protein vangl2 promotes dendrite, spine and glutamatergic synapse formation in the mammalian forebrain. *Molecular Neuropsychiatry*, *2*(2), 107–114.

Rosso, S. B., Sussman, D., Wynshaw-Boris, A., & Salinas, P. C. (2005). Wnt signaling through Dishevelled, Rac and JNK regulates dendritic development. *Nature Neuroscience*, *8*(1), 34–42.

Saito, T., & Nakatsuji, N. (2001). Efficient gene transfer into the embryonic mouse brain using in vivo electroporation. *Developmental Biology*, *240*(1), 237–246.

Shafer, B., Onishi, K., Lo, C., Colakoglu, G., & Zou, Y. (2011). Vangl2 promotes Wnt/planar cell polarity-like signaling by antagonizing Dvl1-mediated feedback inhibition in growth cone guidance. *Dev Elopmental Cell*, *20*(2), 177–191.

Shao, G., Wang, Y., Guan, S., Burlingame, A. L., Lu, F., Knox, R., Ferriero, D. M., & Jiang, X. (2017). Proteomic analysis of mouse cortex postsynaptic density following neonatal brain hypoxia-ischemia. *Developmental Neuroscience*, *39*, 66–81.

Tabata, H., & Nakajima, K. (2001). Efficient in utero gene transfer system to the developing mouse brain using electroporation:

Visualization of neuronal migration in the developing cortex. *Neuroscience*, *103*(4), 865–872.

Tissir, F., & Goffinet, A. M. (2006). Expression of planar cell polarity genes during development of the mouse CNS. *European Journal of Neuroscience*, *23*(3), 597–607.

Tissir, F., & Goffinet, A. M. (2013). Shaping the nervous system: Role of the core planar cell polarity genes. *Nature Reviews Neuroscience*, *14*, 525–535.

Torban, E., Kor, C., & Gros, P. (2004). Van Gogh-like2 (Strabismus) and its role in planar cell polarity and convergent extension in vertebrates. *Trends in Genetics*, *20*(11), 570–577.

Yoshioka, T., Hagiwara, A., Hida, Y., & Ohtsuka, T. (2013). Vangl2, the planner cell polarity protein, is complexed with postsynaptic density protein PSD-95. *FEBS Letters*, *587*(10), 1453–1459.

SUPPORTING INFORMATION

Additional supporting information may be found in the online version of the article at the publisher's website.

How to cite this article: Yasumura, M., Hagiwara, A., Hida, Y., & Ohtsuka, T. (2021). Planar cell polarity protein Vangl2 and its interacting protein Ap2m1 regulate dendritic branching in cortical neurons. *Genes to Cells*, 26, 987–998. https://doi.org/10.1111/gtc.12899